HYDRODYNAMIC STRUCTURE OF A VORTEX RING

D. G. Akhmetov and O. P. Kisarov

Zhurnal Prikladnoi Mekhaniki i Tekhnicheskoi Fiziki, Vol. 7, No. 4, pp. 120–123, 1966

ABSTRACT: Hot-wire anemometry and high-speed motion-picture photography have been used in an experimental study of the structure of a vortex ring in air. The velocity field and streamline pattern have been determined, together with the vorticity distribution. It has been shown that the vorticity is almost entirely localized in the region of the core of the vortex ring and quickly diminishes with distance from the core. Analysis of the experimental results permits a conclusion concerning the nonstationarity of vortex rings.

1. Qualitative picture of vortex ring. Figure 1 shows the streamlines in a coordinate system moving with the vortex [1]. The reference surface consists of the axis of symmetry r = 0 and a certain closed surface dividing the space into two regions: an inner region ($\psi > 0$) and an outer region ($\psi < 0$). In region $\psi > 0$ all the stream surfaces are closed, and the mass of fluid in the volume bounded by the surface $\psi = 0$ moves in space as a unit. This volume is characterized by high stability of motion and there is relatively little change in translational velocity, which indicates that there is little dissipation of energy. This flow pattern is also confirmed by photographic studies [2]. However, these observations do not yield sufficiently convincing conclusions about the velocity field of a vortex ring, the spatial distribution of curl V, and the asymmetry of the streamlines with respect to the plane x = 0 due to viscosity effects. The distribution of curl V is especially important, since a knowledge of this quantity facilitates the finding at a given moment of time of all the other characteristics of the hydrodynamic structure and the dissipation function.

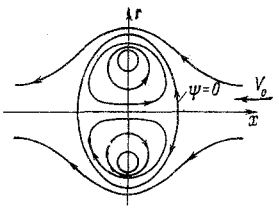

Fig. 1

2. Experimental. Vortex rings in air were obtained by means of the apparatus shown schematically in Fig. 2. A piston 1, whose motion is arrested by a stop, moves at approximately constant velocity (the acceleration length is small as compared with the total displacement of the piston) in a cylindrical tube 75 mm in diameter. At the free end of the cylinder, which ends in a conical nozzle 2, there is formed a vortex ring which subsequently moves so that its axis of symmetry coincides with the axis of the cylinder. The shape of nozzle 2 is selected experimentally so as to give rings with maximum stability of motion. Previous experiments performed by the authors showed that the motion of the vortex may be described as follows: in the first stage beyond the nozzle the flow takes shape, without yet acquiring the form shown in Fig. 1. The path segment corresponding to the first stage is small as compared with the total distance traversed by the vortex. In the second stage the motion of the vortex is characterized by the absence of any visually observable fluctuations; on the other hand, the third stage corresponds to motion with clearly expressed oscillations of the configuration as a whole and intense mixing of the mass originally contained in the region $\psi > 0$ and the masses of the outer region.

The velocity field of the vortex rings was determined using two hot-wire anemometer probes 3 located on the path followed by the vortex in the middle of the section corresponding to the second stage (5.45 nozzle diameters from the nozzle exit). The probe wires were oriented in space so that the signal of one of them gave the absolute velocity $v = \sqrt{v_x^2 + v_r^2}$, this value of v then being used to calculate the velocity components from the signal of the second probe.

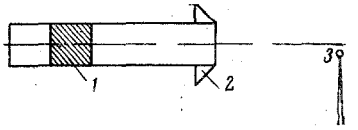

Fig. 2

In order to visualize the motion of the vortex, we introduced into the cylinder pale-gray smoke, which entered the region $\psi > 0$ and made it visible. By means of motion-picture photography we were then able to obtain data on the position of the configuration in space, and by means of time-resolved photography the dependence of the path on time, which was then used to determine the translational velocity.

Apart from the hot-wire anemometer signals, the oscillograms also showed: the time-resolved path of the piston, time marks, and synchropulses that could be used to establish a time correspondence between the anemometer signals and the motion-picture record. The apparatus and the measuring system were controlled from a common switchboard.

3. Velocity field of vortex ring. By analyzing one of the oscillograms it is possible to evaluate the velocity at any point of the cylindrical section r = const. The experiment was repeated five times for each of the sections recorded, so that it was possible to check the stability of the results and use averaged data in the analysis.

We selected eight such sections, the first of which coincided with the axis of symmetry, the interval between sections being 10 mm. To check axial symmetry, two oscillograms, above and below the axis, were obtained for the second section. The signals recorded were indentical, which fully confirms axial symmetry.

The results of the analysis are presented in Figs. 3, 4 in the form of curves relating the dimensionless velocities v_x and v_r and the dimensionless coordinate x. As characteristic kinematic parameters we selected the translational velocity of the vortex v_0 and the diameter of the circular axis of the vortex D. The velocity $v_0 = -1.75$ m/sec was determined from the results of motion-picture and time-resolved

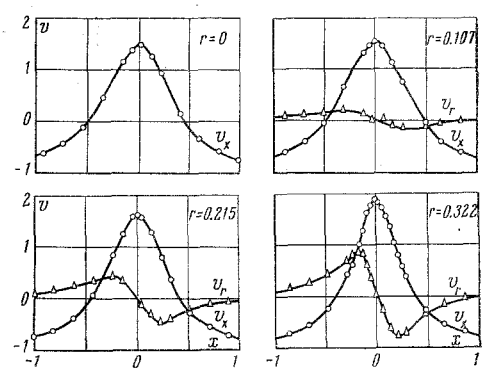

Fig. 3

photography; here it is assumed that during the time interval in which the measurements are made the translational velocity of the vortex is

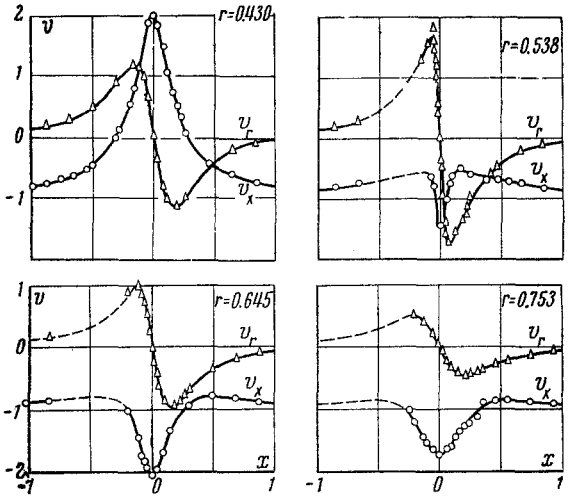

Fig. 4

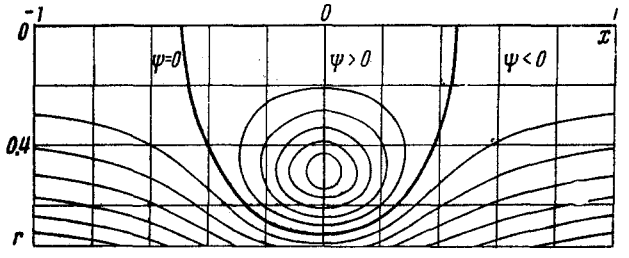

Fig. 5

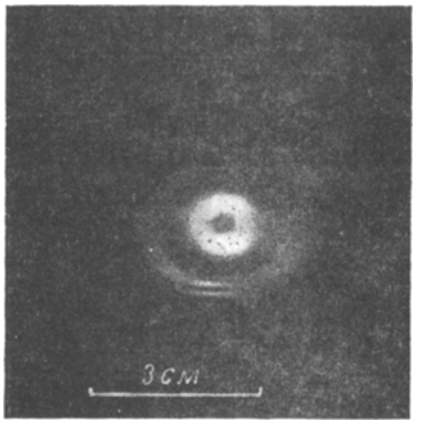

Fig. 6

constant (deviation from v_0 not more than ±1.5%). The circular axis of the vortex is the circle in the region $\psi > 0$ on which the velocities are equal to zero in the coordinate system tied to the vortex ring in translational motion. All the velocities are referred to v_0, the lengths to the vortex diameter D = 98 mm.

It follows from an examination of the graphs that the maximum velocities v_x of each of the sections lie in the plane x = 0 passing through the circular axis of the vortex. In this plane $|v_x| > |v_0|$, except for a region close to the circular axis. At infinity v_x tends to v_0 asymptotically. The maximum values of velocity v_r are localized on the cylinder r = D/2, vanishing at x = 0. At infinity $v_r \to 0$. At x < 0 parts of some of the curves are shown by a broken line. The determination of points on these sections was made difficult by the perturbing influence of the probe holders; however, additional experiments qualitatively confirmed that the curves were of this type. The choice of a characteristic dimension and characteristic velocity makes it possible to calculate the Reynolds number $R = v_0 D/\nu$ for the vortex. In our case $R = 1.08 \cdot 10^4$.

An important characteristic of the hydrodynamic structure of the vortex is the streamline pattern, which can be constructed by numerical integration of the velocity field. In the axisymmetric case the stream function

$$\psi = \int_L r v_r dx - r v_x dr.$$

Here integration is performed along the arbitrary curve L connecting a certain starting point with the point at which the value of ψ is sought. The streamlines for equally spaced values of ψ with a step $\Delta\psi = 0.0175$ are shown in Fig. 5. Here ψ is a dimensionless quantity equal to the ratio of the stream function to the combination $D^2 v_0$. In complete conformity with Reynolds' viewpoint, the zero streamline is closed and divides the eintire space in which flow takes place into two regions. At values of $\psi > 0$ all the streamlines are closed, at $\psi < 0$ they are open curves. As ψ increases, the shape of the closed streamlines approaches that of circles with center on the circular axis of the vortex. For $\Delta r \leq 0.06$, where Δr is the dimensionless distance from the circular axis, the streamlines almost coincide with circles. A certain asymmetry of the streamlines with respect to the plane x = = 0 is observed. The greatest asymmetry is possessed by the streamline $\psi = 0$ (the line $\psi = 0$ cuts off on the r = 0 axis segments whose lengths differ by 10%). The asymmetry is probably attributable to viscosity effects. The shape of the zero streamline is close to an ellipse with corresponding semiaxes, the profile of the streamline being fuller than the profile of this ellipse.

4. Vortex core. An analysis of the velocity curves makes it possible to distinguish a certain toroidal region, the so-called core of the vortex ring. The axis of the torus is the circular axis of the vortex. A characteristic feature of the core is the change in absolute velocity from zero at the center of the core to a maximum value at its edge. Examining the curve representing the velocity v_r as a function of x in the section r = 0.538, we note that close to x = 0 it is linear. This is possible if the section in question passes through a region characterized by rotation at a constant angular velocity. In this case, disregarding to toroidal character of the region, we can write $v_r = \omega x$, $v_x = -\omega(r - 0.5)$, where ω = const is the angular velocity referred to v_0/D. With the help of these expressions it is easy to establish the coordinates of the center of the core, and hence the diameter D and the diameter d of that part of the core which rotates at constant angular velocity. Since the region of the core is toroidal, the actual rotation in any section of the torus cannot have a constant angular velocity, but since the ratio of the dimension of the torus section to the diameter of its circular axis is sufficiently small, the deviation of the true angular velocity from the mean is also small and lies within the limits of experimental error. The angular velocity in the core is equal to 700 sec^{-1}.

Figure 6 shows a slit photograph of the region close to the core. The region is visualized by the smoke particles it contains. At the center of the core the density of the smoke particles is low, then follows an annular region with maximum particle density. This smoke density pattern is easily explained if it is considered that in the region with constant angular velocity the centrifugal force acting on the particles is proportional to the distance from the center of the core, while outside the core it quickly decreases with distance (in the case of a classical cylindrical vortex the centrifugal force outside the core is inversely proportional to the cube of the distance from the center).

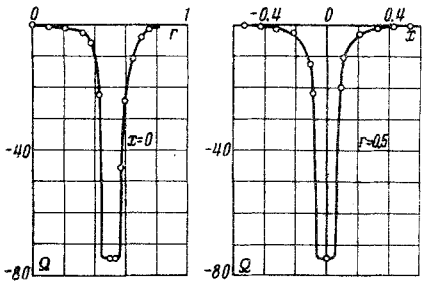

Fig. 7

We have estimated the pressure at the center of the core using the formula for a cylindrical vortex in an ideal fluid $p = p_0 - (1/4)\rho\omega^2 d^2$, where ρ is the density of fluid, and d the diameter of the core, this change in pressure was about 0.03% of p_0.

5. Distribution of vorticity (curl V). Knowing the velocity field, we can construct the distribution of curl V in space. Figure 7 shows the distribution of $\Omega = |\text{curl } V|$ (referred to v_0/D) in the plane x = 0 and along the cylinder r = 0.5.

It is a characteristic feature of this distribution that curl V is almost wholly concentrated in the region of the core; outside the core the value of curl V rapidly declines to zero with increase in distance from the core. On the basis of this vorticity distribution, we may assume that at the initial instant curl V exists only in the core, where it has a constant value. For this case we have the following formula [3] for the translational velocity of a vortex ring:

$$v_0 = \frac{\Gamma}{2\pi D}\left(\ln\frac{8D}{d} - 0.25\right)$$

obtained on the assumption of small d/D. Assuming $T = (\pi/4)d^2\Omega$, we can find the conditional core diameter which would correspond to the experimental values of v_0, D, and Ω. The conditional diameter thus computed is d = 0.166.

On the other hand, the dimension corresponding to twice the distance from the center of the core to the points were the velocity acquires maximum values is found in the interval d = 0.155–0.180. Thus, the formula for the translational velocity of a vortex ring in an ideal fluid is in good agreement with the actual motion of a vortex ring at a moment sufficiently close to the moment of formation.

6. Stationarity of the vortex ring. For the case of motion of vortex rings in an ideal fluid we can write the stationarity condition [3] in the form

$$|\text{curl } V| = rf(\psi), \quad \text{or} \quad \frac{\partial^2\psi}{\partial x^2} + \frac{\partial^2\psi}{\partial r^2} - \frac{1}{r}\frac{\partial\psi}{\partial r} = r^2 f(\psi), \qquad (6.1)$$

where $f(\psi)$ is an arbitrary function of ψ. Using this condition, from the experimental data of Figs. 5 and 7 it is easy to establish that the stationarity condition is not satisfied.

For example, the streamline $\psi = 0.105$ (Figs. 5 and 7) gives at x = = 0 $r_1 = 0.35$, $\Omega_1 = -4$ and $r_2 = 0.618$, $\Omega_2 = -16$, respectively. Consequently, $f(\psi)$ in (6.1) takes the values $f_1 = -11.4$ and $f_2 = -25.9$. However, the stationarity condition (6.1) requires the constancy of $|\text{curl } V|/r$ along the streamline ψ = const. Thus, the vortex distribution obtained will not be stationary for the model of an ideal fluid.

The authors thank V. K. Sheremetov and V. A. Kosinov for their assistance.

REFERENCES

1. O. Reynolds, "On the resistance encountered by vortex rings, etc." Brit. Ass. Rep., Nature, vol. 14, p. 477, 1876.

2. R. H. Magarvey and C. S. Maclatchy, "The formation and structure of vortex rings," Canad. J. Phys., vol. 42, No. 4, 1964.

3. H. Lamb, Hydrodynamics [Russian translation], OGIZ-Gostekhizdat, 1947.

19 January 1966 Novosibirsk